

PalaeoMath 101

Distances, Landmarks and Allometry

This column marks a slight change in topic for the *PalaeoMath* series. Up to now we've been considering standard bivariate (regression) and multivariate data analysis procedures, techniques that can be applied to a broad range of data. While it is true that in all those essays I've used morphological examples as a basis for explaining the procedures, and while they all work well with morphological data, their use is by no means so restricted. At present you're more likely to see PCA, PCoord, MDS, etc. used to analyze non-morphological than morphological datasets.

This wasn't always the case. Through the mid-1980's these multivariate procedures were used routinely to analyze morphological data. They even formed a 'school' of morphological data analysis called 'multivariate morphometrics', coined by Robert Blackith and Richard Reyment (1971). So, what happened? As it turned out the multivariate approach to morphometric analysis was synthesized with another prominent school of morphometric analysis—the deformational approach—in the mid-1980s, largely through the work of Fred Bookstein, but with important contributions by a number of others. This new approach to the analysis of morphological data crystallized into what is now termed 'geometric morphometrics' with the publication Bookstein's (1991) treatise on the topic. Now most morphometric studies are undertaken using the methods of geometric morphometrics. Although it is by no means uncommon to see articles published using the older multivariate morphometric approaches, those are dwindling as more researchers become aware of the power of geometric morphometrics and learn how to use the software that has been developed to implement the various geometric approaches. Accordingly, we will now turn our attention to this important group of methods for handling the analysis of morphological data.

The geometric morphometric approach is bound up with the concept of the landmark. In the context of geometric morphometrics a landmark is defined as 'a specific point on a biological form or image of a form located according to some rule. Landmarks with the same name, homologues in the purely semantic sense, are presumed to correspond in some sensible way over the forms of a data set.' (Slice et al., 2008). There are a number of alternative definitions of the term (e.g., Bookstein et al. 1985; Bookstein 1991; Dryden and Mardia 1998; Zelditch et al. 2004), but this one seems the most general to me.

Note the careful use of the term 'homology'. Landmarks are always assumed to represent corresponding parts of locations on the body, but they do not always—nor always need to—represent formal homologues in the biological sense of that term. Indeed, in the vast majority of cases landmarks can't be demonstrated to represent formal biological homologues. The concept of a homologue refers to a biological structure in its entirety (e.g., the eye of a fish, amphibian, reptile, bird, and mammal), not an isolated mathematical point defined on the basis of that structure's geometry (e.g., centre of the iris opening), however convenient that point may be for making quantitative comparisons. This centre of the iris is a good example of the logical complications one can get into by (needlessly) becoming embroiled in assertions about landmark homology insofar as this point has been used routinely in fish morphometric studies, but in fact corresponds to ... nothing. There is no structure at the centre of the iris opening to argue the homology of. It is simply an abstract point that is as good as any other for representing the position of the eye relative to other morphological structures. It is the eye that is homologous across vertebrate taxa, not a constructed point in the centre of an opening within that structure (see MacLeod 1999 for additional examples). Landmark points are used to locate the positions of structures relative to other structures whose positions are themselves represented by other landmark points. This more generic view of what landmarks are, aside from being logically defensible, also has the virtue of being consistent with the specification of different types of landmarks (e.g., semilandmarks, constructed landmarks) as well as with both historical and contemporary practice.

The representation of morphology by landmarks has both trivial and profound implications (Fig. 1). Note that in previous essays we represented morphology by the simple device of measuring linear distances on the specimen, as we would with a set of callipers or using a ruler on a photograph. This resulted in a table of values; with sets of distances for different specimens typically organized into a matrix in which the rows represent specimens and the columns represent variables: the set of corresponding distances collected from each specimen. Of course the irony of this procedure with respect to landmarks is that, in order to know

what distances to measure we needed to define the end-points of the distances which are—landmarks. Thus, we've actually been working with landmark data throughout these essays; we've just been focusing on the distances between landmarks, not the landmarks themselves.

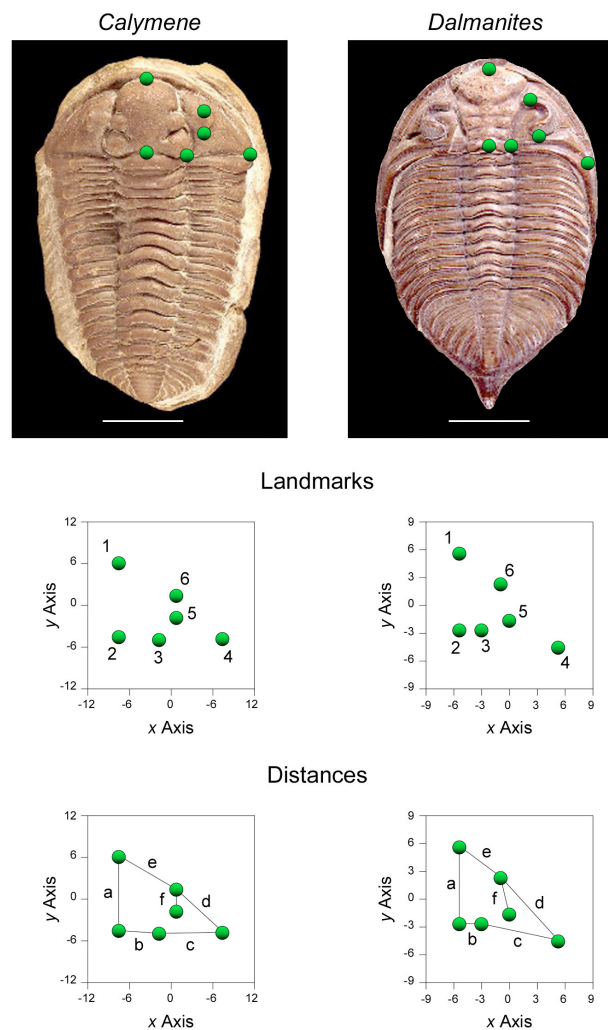


Figure 1. Alternative schemes for measuring size and shape differences between the cranidia of two trilobites. Upper row: images of *Calymene* and *Dalmanites* specimens with six cranidial landmarks indicated (see text for definition). Scale bars: 11.87 and 8.20 mm, respectively. Middle row: geometry of landmark distributions in a scaled, mean-centred coordinate system. Note the obvious shape differences. In the lower row the landmarks have been joined by a series of chords the lengths of which represent inter-landmark distances. However, spatial relations between these chords are able to be appreciated only because we have retained the information encoded in the landmarks. These distances, as distances, are more accurately depicted as a simple table of values (Table 1).

Figure 1 illustrates the difference this makes. Here, aspects of trilobite cranidial shape have been represented by the six landmarks: 1: anterior central glabellar margin, 2: posterior central glabellar margin, 3: right posterior glabellar margin, 4: right lateral posterior fixigena terminus, 5: posterior eye margin, 6: anterior eye margin.¹ In the middle row of the diagram locations of these six landmarks have been placed into a scaled, mean-centred coordinate system. Note the obvious shape differences. In the lower row the landmarks have been joined by a series of chords the lengths of which represent inter-landmark distances. However, spatial relations between these chords are able to be appreciated only because we have retained the information encoded in the landmarks. These distances, as distances, are more accurately depicted as a simple table of values (Table 1).

¹ Because trilobites are bilaterally symmetrical only the right half of the cranidium has been measured.

Table 1. Scaled inter-landmark distance values for the trilobite cranidia. All values in mm.

Distance	<i>Calymene</i>	<i>Dalmanites</i>
<i>a</i>	11.675	8.985
<i>b</i>	6.239	2.346
<i>c</i>	10.343	8.683
<i>d</i>	11.421	10.036
<i>e</i>	9.753	5.450
<i>f</i>	3.551	4.116

As you can see, if all we had was the information included in Table 1 it would be very difficult to infer the correct relative positions of the landmarks. Each landmark is located relative to others by only two distances, with the exception of landmark 5, which is located by only one. The distance values obtained from each trilobite image are consistent with a wide variety of landmark configurations, only one of which is correct.

Contrast this with the situation for the landmark coordinate locations (Table 2).

Table 2. Scaled, mean-centred landmark coordinate point data for the trilobite cranidia. All coordinates in mm.

Landmark	<i>Calymene</i>		<i>Dalmanites</i>	
	x	y	x	y
1	-6.746	8.238	-3.926	6.595
2	-6.746	-3.438	-3.666	-2.386
3	-0.519	-3.827	-1.323	-2.256
4	9.794	-4.605	7.137	-4.208
5	2.400	0.065	1.540	-0.824
6	1.816	3.567	0.239	3.080

Because the coordinate point locations are referenced to linear distances along independent *x* and *y* axes they record the position of each landmark relative to every other landmark precisely and succinctly. The data in Table 2 are geometrically equivalent to having a table of all possible inter-landmark distances (15 distances in all for 6 landmarks, see Fig. 2). But in terms of reconstructing the geometry of the landmark points they are even better as all the coordinates are uniquely referenced to a single location—the origin of the coordinate system—thus obviating the need for inferential landmark reconstruction procedures. The coordinate-point representation is also far better from an analytic point of view in that many of the possible inter-landmark distances are redundant owing to their similarity in length and orientation. The penalty paid for this increase specificity, however, is an increase in the number of variables necessary to fully represent the forms. Once we have our data in landmark form we can easily compare the results of distance and landmark-based morphometric analyses to assess the advantages of using landmarks to measure morphology.

To make use of landmarks the first issues we need to tackle are position and orientation. Because inter-landmark distances represent simple magnitude, or scalar, variables, so long as we don't make a mistake assembling our data matrix (e.g., put different measurements in the same column or the same measurements in different columns) it doesn't matter where the specimen was or how it was oriented when we took the measurements. The distance values will be the same regardless. Not so for landmark variables. Since landmarks encode the fundamental geometry of forms, differences in specimen position and orientation are part of landmark data. If we are interested in analyzing differences in specimen position or orienta-

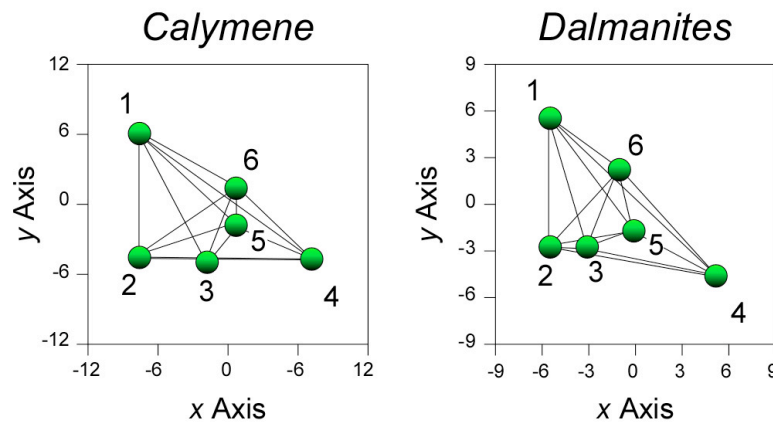


Figure 2. All pairs of distances between the six trilobite landmarks. See text for discussion.

tion, that's great. For example, if we wanted to analyse the distribution of trilobites across a bedding plane and/or their orientation relative to the prevailing current direction, raw landmark data would be fine. But if we're not interested in differences between specimens that have to do with their positions and/or orientations during measurement, we need to correct for these factors in order to bring the distribution of landmarks into positional and orientational conformity. Fortunately, there are a couple of easy equations we can use to do this.

The first step in this procedure is to decide on a reference orientation: some standard configuration of landmarks all specimens could be brought to. For the trilobite data an obvious reference orientation would be landmark data that are mean centred with the mid-line chord (between landmarks 1 and 2 in the middle part of Fig. 1) perpendicular to the x-axis and parallel to the y-axis. This is more-or-less the standard orientation for trilobite illustrations and is shown for the example *Calymene* and *Dalmanites* landmarks in Figure 1. But even these data are slightly out of alignment (note difference in the *Dalmanites* x-coordinate values for landmarks 1 and 2). Strict conformity can be gained by (1) reversing the x and y columns of the data², (2) centring the landmark distribution on landmark 2, (3) calculating the slope of the mid-line chord, (4) calculating the angle between the mid-line chord and the x-axis ($= 0^\circ$), and (5) rigidly rotating the entire landmark distribution so that landmark 1 lies on the x-axis, and landmark 2 lies at the origin, of the coordinate system. The procedure for making these calculations is detailed in the *Palaeo-Math 101-2* spreadsheet and the equations needed for implementing steps 4 and 5 are listed below.

$$\text{Step 4} \quad \tan^{-1} \theta = \frac{m_2 - m_1}{1 + m_1 m_{21}} \quad (14.1)$$

$$\text{Step 5} \quad \begin{aligned} v_1 &= x \cos(\theta) + y \sin(\theta) \\ v_2 &= -x \sin(\theta) + y \cos(\theta) \end{aligned} \quad (14.2)$$

In equation 14.1 m_1 and m_2 represent the slopes of x-axis ($= 0^\circ$), and the mid-line chord.³ Once the correct rotated values have been obtained the x and y columns can be re-transposed and the entire landmark dataset re-centred about the new mean x and mean y

² This step rotates the landmarks by 90° and is needed with these data to avoid complications arising with the calculation of an infinite mid-line slope for some specimens.

³ See the first essay in this series (Newsletter 55) for instructions on how to calculate a slope.

values (= centroid). Table 3 shows the results of these calculations for the two example trilobite genera.

Table 3. Scaled, rotated, and mean-centred landmark coordinate point data for trilobite crania. All coordinates in mm.

Landmark	<i>Calymene</i>		<i>Dalmanites</i>	
	x-rotated	y-rotated	x-rotated	y-rotated
1	-6.746	8.238	-3.734	6.706
2	-6.746	-3.438	-3.734	-2.279
3	-0.519	-3.827	-1.388	-2.217
4	9.794	-4.605	7.012	-4.413
5	2.400	0.065	1.516	-0.869
6	1.816	3.567	0.328	3.072

Now that we have our landmark data in a form suitable for comparison we can perform a PCA analysis on these data and compare the results of that with a PCA of the inter-landmark distance data as shown in Figure 1 and Table 1. Eighteen of our 20 trilobite images are suitable for the collection of these data (names shown in Fig. 3).

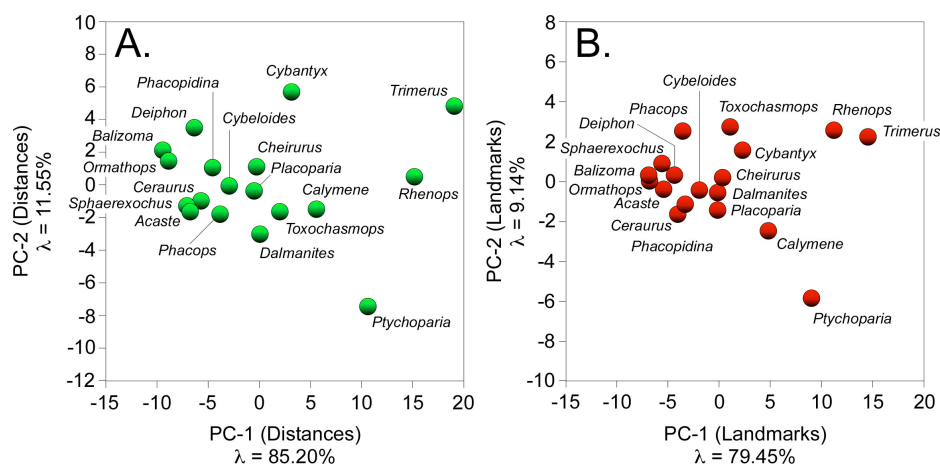


Figure 3. Ordination of trilobite crania inter-landmark scaled distances (A) and scaled, rotated landmark positions (B) in the space of the first two principal components of the respective datasets' covariance matrices.

Ordinations of the two datasets using the first two principal component axes (Fig. 3) are broadly similar, as would be expected. The amount of variation represented by PC-1 and PC-2 relative to the total variation is slightly lower in the case of the landmark-based analysis. This is also expected as that dataset contains twice as many variables as the inter-landmark distance dataset.

In both cases the PC-1 axis appears to ordinate taxa by size, with small individuals (e.g., *Balizoma*, *Ormathops*) projecting to positions low on the axis and large individuals (e.g., *Rhenops*, *Trimerus*) projecting to positions high on the axis. Close inspection of the diagrams shows the taxa are all in precisely the same rank order along PC-1, confirming the interpretation of this axis as a size index. However, the two analyses differ strongly in terms of the PC-2 ordination. Since the landmark-based dataset has the higher geometric information content this result suggests the distance data are masking both similarities and differences among taxa and so presenting a somewhat biased picture of the true state of morphological affairs. In other words, the switch to representation of the same geometries by landmarks made a difference not in terms of the assessment of size similarity, but in the assessment of shape

similarity. This difference is most readily appreciated by inspecting the orientation of the principal component axes relative to the original variables (Table 4).

Table 4. Principal component loadings for distance-based (left) and landmark-based (right) covariance matrices.

Distance ^a	PC-1	PC-2		Landmark	PC-1	PC-2
<i>a</i> (1-2)	0.646	0.453		1x	-0.315	0.191
				1y	0.600	0.610
<i>b</i> (2-3)	0.222	0.105		2x	-0.315	0.191
				2y	-0.240	0.124
<i>c</i> (3-4)	0.323	-0.516		3x	-0.020	0.141
				3y	-0.248	0.104
<i>d</i> (4-6)	0.444	-0.568		4x	0.419	-0.468
				4y	-0.288	-0.300
<i>e</i> (6-1)	0.454	0.329		5x	0.175	-0.185
				5y	0.002	-0.237
<i>f</i> (5-6)	0.160	-0.292		6x	0.055	0.131
				6y	0.174	-0.302

^aNumbers in parentheses refer to distance-defining landmarks.

The distance-based results (Table 4, left side) are highly reminiscent of the example given previously in the column on principal component analysis (see Newsletter 59). All loadings on PC-1 are positive but unequal indicating this axis represents allometric size change.⁴ The theoretical value of a six-variable isometric axis is 0.408. Accordingly, distance *a* shows strong positive allometry, distances *d* and *e* weak positive allometry, and the remainder weak negative allometry. The orientation of these distances (see Fig. 1) suggests the glabellar mid-line is disproportionately longer in large sized specimens with the overall cranial length slightly longer than would be expected under a model of strictly isometric size change. That fact that distances located in the posterior portion of the structure are negatively allometric also suggests a slight narrowing of the cranial shield accompanied by a strong reduction in eye size.

Whereas the PC-1 axis represents mixed size and shape variation, the PC-2 axis represents pure shape variation as indicated by its mix of positive and negative loadings. Here, taxa scoring high on PC-2 exhibit large values for the glabellar mid-line and anterior cranial shield distances and small values for distances attached to landmark 4 in the postero-lateral region. Eye size is also negatively correlated with an increase in PC-2 score.

While this might appear to be a lot of information, note that, for the most part, each distance must be interpreted in isolation from every other. High scores on PC-1 and PC-2 mean small eyes, low scores large eyes. But how is the position of the eye changing with respect to the

⁴ Readers who recall the previous essay on the analysis of univariate and multivariate allometry will note—possibly with some surprise—that I have not log-transformed the original distance data. The purpose of the log-transform in allometric studies is to enable linear regression methods to estimate non-linear regression models (e.g., logistic growth curves). While this is the classic procedure for allometric analyses, the analysis of non-transformed data is also appropriate for allometric investigations insofar as (1) most morphological data are not demonstrably non-linear and (2) the principle of allometry pertains to any comparison between size and shape data, not just comparisons between log-transformed variables. In the end the decision to employ a log-transformation should be dictated by the purpose of the analysis, the data, and characteristics of the data analysis method. Allometric theory is equivocal with respect to this issue. See Klingenberg (1996) for additional discussion.

position of the glabella? Is the glabella pushing out anteriorly, pushing back posteriorly, or both as size increases across these taxa? These questions are very difficult to answer from the distance-based results because each distance confounds two distinct sources of shape-change data—change in the x -axis direction and change in the y -axis direction—despite the fact that *information about these directions of shape change was collected in order to calculate the inter-landmark distance values.*

Contrast this with the much more complex and information-rich summary provided by the landmark data (Table 4, right side). The first thing to notice here is that the simple multivariate allometric interpretation of PC-1 doesn't necessarily apply to landmark data. This is indicated by the mixture of positive and negative loading values on the PC-1 axis. A mixed PC-1 loading pattern is characteristic of many landmark datasets and is a reflection of the fact that scalar distances between landmark points can increase at the same time as either x or y coordinate values *decrease* (e.g., as the orientation of the distance becomes either more or less aligned with the x or y axis).

As we noted in interpreting the distance and landmark data ordinations along PC-1, the major axis of variation for the landmark dataset appears to reflect size differences among the taxa despite the fact that the loading pattern does not identify it as an allometric size axis. This somewhat counter-intuitive result has occurred in the example analysis because the two landmark variables that load most strongly onto PC-1 (1y and 4x) are also the variables with the largest mean values (as well as the largest variances) by a considerable margin. Also note that these positive loadings are much higher than any of the negative loadings for the other variables on PC-1. Geometrically, this means that, for these specimens, the glabellar mid-line length and lateral width in the region of posterior extra-glabellar cranial shield are exhibit both large displacements from other landmarks and increase with increasing overall size at disproportionately higher rates than those of any other variables. These two particular aspects of the morphological variation are dominantly responsible for the perceived size increase among the taxa in our sample. But how can this be when the distance-based results clearly identified distances a , d , and e as being the most positively allometric? A moment's reflection reveals the reason and, along with it, the power of the landmark approach.

The disproportionately high loading on landmark 1y indicates that migration of landmark 1 in the anterior direction is the shape change most responsible for size differences among taxa. This is reflected perfectly in the distance results by the high loadings assigned to distances a and e , both of which share landmark 1. In the distance-based results it was ambiguous whether the cranial mid-line was getting longer because of a change in the relative positions of landmarks 1, 2 or both. The landmark-based results neatly resolve this ambiguity. The focus of change is landmark 1 and the direction of change is along the y -axis (anterior-ward). Similarly, distance e has a high loading on the distance-based PC-1 because that distance is being dragged out by the anterior-ward migration of landmark 1. To be fair, there is a slight anterior-ward migration in landmark 6 as well, but its rate is far outstripped by that of landmark 1. As for landmark 2, the distance between it and the origin is actually decreasing with increasing cranial size. Thus, the whole glabellar mid-line is shifting anterior-ward relative to the other landmarks.

Along the x -axis, it's more-or-less the same story. Landmark 4 is shifting its position strongly in a lateral direction, away from the mid-line and migrating anteriorly at a slightly higher rate than landmark 2. This shift accounts for the high positive loading on distance d in the distance-based results. Moreover, inspection of loadings for landmark 2 also explains the negative allometry shown for distances b and c as that landmark (along with landmark 1) is migrating toward the y -axis (= line containing the form centroid) as size increases. In other words, within this sample the cranidia are becoming disproportionately longer (via anterior-ward migration of landmark 1) and narrower via migration of landmarks 1 and 2 inboard in the lateral direction), and the lateral portion of the cranial shield getting disproportionately wider (via outboard lateral migration of landmark 4) with increasing cranial size.

Now let's have a look at the eye. The distance-based results tell us only that the eye is getting smaller with increasing cranial size. The landmark-based results confirm it's getting relatively smaller (difference between loadings on both 5y-6y vs. 1y, and 5x-6x, vs. 4x), but also that it's shifting to a position farther back on the cranial shield (difference between 6y and 1y loadings) with a posterior margin placed closer to the glabella (difference between 5x and 4x loadings). In addition, differences in the eye landmark loadings themselves indicate its orien-

tation is changing such that the chord joining the anterior and posterior landmarks is rotating anti-clockwise with increasing cranial size. And all this is just the interpretation of landmark PC-1!

With respect to landmark PC-2 we note the broad regional distinctions among the landmarks with 1, 2, and 3 all migrating away from the origin in both x and y dimensions (1y very strongly so), and landmarks 4 and 5 migrating toward the origin. This represents a subdominant pattern of cranial lengthening—differentially focused in the anterior region of the form—and lateral compression, accompanied with strong reduction in eye width and further rotation of the eye landmarks.

Admittedly the previous three paragraphs are a bit dense and abstract. But I hope the take-home message is clear. Analysis of landmark coordinate positions enables far more geometric information to be incorporated into an analysis—and supports far less ambiguous interpretation of the results—than the analysis of inter-landmark distances. In fact, the amount of information that can be gained from an analysis of landmarks is so large that much of the effort in developing geometric morphometric techniques has been spent developing mathematical tools to enable interpretations like those above to be made not by inspecting tables of numbers (as we have done here and as must be done with all standard multivariate data-analysis techniques), but by inspecting new types of ordination diagrams that summarize the complex and subtle geometric information in an easy-to-interpret graphical manner. It is to these methods with their accompanying graphics that we will turn our attention in future essays.

Most presentations of geometric morphometrics begin simply by defining landmarks and then diving into the subject of shape coordinates. Here I've tried to focus a bit more on the link between distance-based morphometrics and landmark-based morphometrics so that when we get to shape coordinates (next column) the distinction between old-style multivariate morphometrics and new style geometric morphometrics won't seem so abrupt. Although the transition between multivariate and geometric morphometrics occurred in a sufficiently short space of time that those of us who lived through it often speak of it as a 'revolution', the revolution actually had quite deep roots. Nevertheless, the translation and rotation methods I've outlined in this essay are based on equations that were developed for general geometric purposes, not specifically for morphometrics. These are not considered part of the established corpus of geometric morphometrics methods as they have been superseded by methods that allow greater control of size and shape aspects of the data. Instead, they represent precursor concepts and tools that form the (largely unacknowledged) background against which the discussion of more mainstream geometric morphometric techniques should be viewed. As such, there are no 'canned' programmes for performing the standardizing rotations I have illustrated in this essay other than the *Palaeo-Math 101-2* spreadsheet.

Norman MacLeod

Palaeontology Department, The Natural History Museum
N.MacLeod@nhm.ac.uk

REFERENCES

- BLACKITH, R. E. and R. A. REYMENT. 1971. *Multivariate morphometrics*. Academic Press, London. 412 pp.
- BOOKSTEIN, F., B. CHERNOFF, R. ELDER, J. HUMPHRIES, G. SMITH, and R. STRAUSS. 1985. *Morphometrics in evolutionary biology*. The Academy of Natural Sciences of Philadelphia, Philadelphia. 277 pp.
- BOOKSTEIN, F. L. 1991. *Morphometric tools for landmark data: geometry and biology*. Cambridge University Press, Cambridge. 435 pp.
- DRYDEN, I. L. and K. V. MARDIA. 1998. *Statistical shape analysis*. J. W. Wiley, New York. 376 pp.

- KLINGENBERG, C. P. 1996. *Multivariate allometry*. In L. F. Marcus, M. Corti, A. Loy, G. J. P. Naylor, and D. E. Slice, eds. *Advances in morphometrics*. Plenum Press, New York. 23–49 pp.
- MACLEOD, N. 1999. Generalizing and extending the eigenshape method of shape visualization and analysis. *Paleobiology*, **25(1)**, 107–138.
- SLICE, D. E., F. BOOKSTEIN, L., and F. J. ROHLF. 2008. *A Glossary for Geometric Morphometrics*. University of New York, Stony Brook. <http://life.bio.sunysb.edu/morph/>.
- ZELDITCH, M. L., D. L. SWIDERSKI, H. D. SHEETS, and W. L. FINK. 2004. *Geometric morphometrics for biologists: a primer*. Elsevier/Academic Press, Amsterdam. 443 pp.

Don't forget the *Palaeo-math 101-2* web page, now at a new home at:
http://www.palass.org/modules.php?name=palaeo_math&page=1